



## Static liquefaction behavior of saturated fiber-reinforced sand in undrained ring-shear tests

Jin Liu<sup>a,b,c</sup>, Gonghui Wang<sup>a,\*</sup>, Toshitaka Kamai<sup>a</sup>, Fanyu Zhang<sup>a</sup>, Jun Yang<sup>d</sup>, Bin Shi<sup>b</sup>

<sup>a</sup> Research Centre on Landslides, Disaster Prevention Research Institute, Kyoto University, Gokasho, Uji, Kyoto 611-0011, Japan

<sup>b</sup> School of Earth Sciences and Engineering, Nanjing University, Nanjing 210093, China

<sup>c</sup> School of Earth Sciences and Engineering, Hohai University, Nanjing 210098, China

<sup>d</sup> Department of Civil Engineering, The University of Hong Kong, Hong Kong, China

### ARTICLE INFO

#### Article history:

Received 10 October 2010

Received in revised form

25 February 2011

Accepted 3 March 2011

Available online 11 April 2011

#### Keywords:

Static liquefaction

Fiber-reinforced sand

Undrained shear

Ring-shear test

### ABSTRACT

The problem of static liquefaction of sand is nowadays a classical soil mechanics subject. Using a ring-shear apparatus, we explore the possibility of fiber reinforcement as a new method to improve the liquefaction resistance of sand. In order to understand the effect of the fiber content and sand density on the static liquefaction behavior of fiber-reinforced sand, a series of undrained ring-shear tests were carried out on saturated samples with different fiber content and sand density, and the test results and mechanisms of fiber reinforcement were then analyzed. The results indicate that the undrained shear behavior of fiber-reinforced loose samples is not greatly influenced by the presence of fiber, but for medium dense and dense samples, the presence of fiber clearly affects their undrained behavior. Untreated specimens showed a continuous decrease in shear resistance after failure, while the specimens treated with fiber showed fluctuations even after shear failure, and these fluctuations become stronger with increasing fiber content. The peak shear strength increases with the fiber content, especially in dense specimens. After shearing, all the fiber-reinforced and untreated dense samples maintained structural stability, while the unreinforced loose samples showed a completely collapse of structure. The presence of fibers may thus limit or even prevent the occurrence of lateral spreading that is often observed in unreinforced sand.

© 2011 Elsevier Ltd. All rights reserved.

### 1. Introduction

The problem of static liquefaction of saturated sand is nowadays a classical soil mechanics subject. Castro (1969) found that sudden increases of pore water pressure, induced by monotonic shearing under undrained conditions, lead to the liquefaction of sand layers. Sand liquefaction can result in landslides, subsidence of foundations, damage to earth structures, lateral movement of structures resting on soil, and disruption of services. It is thus important to consider the liquefaction potential of dams, embankments, slopes, foundation materials and placed fills (Krishnaswamy and Isaac, 1994). At present, the methods most commonly adopted to prevent liquefaction are densification, draining and soil reinforcement (Krishnaswamy and Isaac, 1994). Nevertheless, densification of deep deposits and draining is often ineffective and require suitable field equipment, so soil reinforcement has been considered

recently (Vercueil et al., 1997; Li and Ding, 2002; Unnikrishnan et al., 2002; Boominathan and Hari, 2002; Diambra et al., 2010).

Soil reinforcement using tension-resisting material is an attractive method of improving the property of soils in geotechnical engineering and other fields (Rowe and Li, 2002; Rowe and Taechakumthorn, 2008; Li and Rowe, 2008; Long et al., 2007). Distributed fiber used as a new reinforcing material has recently become a focus of intense interest (Maher and Ho, 1993; Santoni and Webster, 2001; Santoni et al., 2001; Zornberg, 2002; Consoli et al., 2003, 2007, 2009a,b; Heineck et al., 2005; Park and Ann Tan, 2005; Yetimoglu et al., 2005; Diambra et al., 2007, 2008, 2010; Michalowski, 2008; Tingle et al., 2002; among others). Compared with conventional reinforcement materials (strips, geotextile, geogrid, etc.), the mixing of discrete fibers with a soil mass is simple and quite similar to adding other mixtures such as cement and lime. One of the primary advantages of randomly distributed fibers is the absence of potential planes of weakness that can develop parallel to oriented reinforcement (Tang et al., 2007). A number of conventional triaxial tests, unconfined compression tests, and direct shear tests on this subject have been

\* Corresponding author. Tel.: +81 774 38 4839; fax: +81 774 384300.  
E-mail address: [gonghui.wang@gmail.com](mailto:gonghui.wang@gmail.com) (G. Wang).

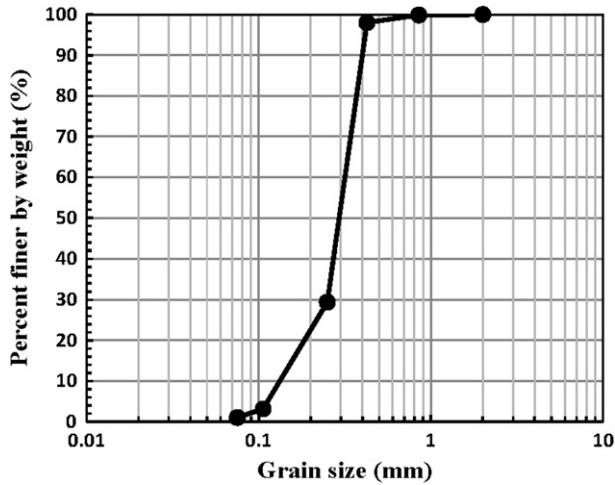


Fig. 1. Grain size distribution of Silica sand No.6 (S6).

conducted by several investigators in the last few decades (Al Refeai, 1991; Maher and Ho, 1994; Krishnaswamy and Isaac, 1994; Ranjan et al., 1994, 1996; Li et al., 1995; Wasti and Butun, 1996; Prabakar and Sridhar, 2002; Kaniraj and Gayathri, 2003; Yetimoglu and Salbas, 2003; Yetimoglu et al., 2005; Tang et al., 2007; Chen and Loehr, 2009; Consoli et al., 2009a; Sadek et al., 2010 among others). Their research has demonstrated that shear strength is increased and post-peak strength loss is reduced when discrete fibers are mixed with the soil. The effectiveness of the reinforcement is influenced by the properties of the fiber, including type, volume fraction, length, aspect ratio, modulus of elasticity, and orientation, and also soil characteristics including particle size, shape, and gradation, as well as stress level and density. Fiber orientation has an important influence on the mechanical properties of fiber-reinforced soils (Jewell and Wroth, 1987; Palmeira and Milligan, 1989; Michałowski and Cermák, 2002). However, the most common procedure for preparing reinforced specimens, moist tamping, leads to a preferred subhorizontal orientation of fibers (Diambra et al., 2008).

Most previous studies have focused on the strength and deformation characteristics of fiber-reinforced soil. The liquefaction behavior of reinforced soils has received recent attention for assessing the usefulness of fiber reinforcement as a new way to prevent soil liquefaction. When sand or clay are reinforced with short fibers under cyclic loading, the presence of fiber leads to an increase in the number of cycles required to cause liquefaction under undrained loading conditions (Noorany and Uzdavines, 1989; Maher and Woods, 1990; Vercueil et al., 1997; Li and Ding, 2002; Unnikrishnan et al., 2002; Boominathan and Hari, 2002; Krishnaswamy and Isaac, 1994). Static liquefaction behavior of fine sand reinforced with discrete crimped polypropylene fibers in both triaxial compression and triaxial extension undrained tests are presented by Ibraim and Fourmont (2007) and Ibraim et al. (2010).

In this paper, we present a method for studying the static liquefaction behavior of sand reinforced with randomly distributed short polypropylene fiber (12 mm long) using a ring-shear apparatus (DPRI-Ver.5). In order to understand the effect of the fiber content and sand density on the liquefaction behavior of the fiber-

Table 2  
List of the ring-shear tests performed.

Test	$P_f$ (%)	$e_s$	$\rho_s$ (g/cm <sup>3</sup> )	Dr (%)	Density grade	Normal stress (kpa)	Saturation degree $B_D$	Comment
T1	0	1.054	1.285	12.6	L	200	0.96	✓
T2	0.2	1.061	1.281	11.1	L	200	0.68	Unsaturated
T3	0.2	1.057	1.283	12.0	L	200	0.98	✓
T4	0.4	1.064	1.279	10.3	L	200	0.98	✓
T5	0.6	1.043	1.292	15.3	L	200	0.97	✓
T6	0.8	1.069	1.276	9.3	L	200	0.82	Unsaturated
T7	0.8	1.094	1.261	3.5	L	200	0.97	✓
T8	0	0.970	1.340	31.8	M	200	0.96	✓
T9	0.2	0.977	1.335	30.3	M	200	0.95	✓
T10	0.4	0.968	1.341	32.3	M	200	0.81	Unsaturated
T11	0.4	0.973	1.337	31.0	M	200	0.98	✓
T12	0.6	0.971	1.339	31.6	M	200	0.97	Drain
T13	0.6	0.976	1.335	30.4	M	200	0.95	✓
T14	0.8	0.978	1.334	29.9	M	200	0.98	✓
T15	0	0.873	1.409	53.8	D	200	0.95	✓
T16	0.2	0.879	1.405	52.5	D	200	0.78	Unsaturated
T17	0.2	0.868	1.413	55.0	D	200	0.85	Unsaturated
T18	0.2	0.884	1.401	51.3	D	200	0.96	✓
T19	0.4	0.865	1.416	55.8	D	200	0.97	✓
T20	0.6	0.909	1.382	45.6	D	200	0.95	✓
T21	0.8	0.931	1.367	40.6	D	200	0.98	✓

Note: L = loose; M = moderate dense; D = dense.

reinforced sand, a series of undrained ring-shear tests were carried out on saturated samples with different percentages of fiber content and sand density. The test results and reinforcement mechanisms are discussed.

## 2. Materials and experimental procedure

### 2.1. Materials

For this study, we used Silica sand No.6 (S6). This sand, which is used for building, is made from silica sandstone by grinding and comprises subangular to angular quartz. Its specific gravity is approximately  $G_s = 2.64$ . The maximum and minimum dry densities are measured as  $\rho_{max} = 1.58$  and  $\rho_{min} = 1.25$  g/cm<sup>3</sup>, respectively, following the procedures of ASTM. The maximum and minimum void ratios are  $e_{max} = G_s/\rho_{min} - 1 = 1.108$  and  $e_{min} = G_s/\rho_{max} - 1 = 0.674$ , respectively. The grain size distribution of sand S6 is presented in Fig. 1. S6 has a mean grain size,  $D_{50} = 0.30$  mm, a coefficient of uniformity,  $C_u = D_{60}/D_{10} = 2.29$ , and a coefficient of gradation,  $C_g = (D_{30})^2/(D_{10}D_{60}) = 1.34$ . The properties of the short polypropylene fibers used in this study are given in Table 1. The percentage of fiber is defined herein as a proportion of dry weight of sand  $P_f = (W_f/W_s) \times 100$ , where is  $W_f$  the weight of fibers and  $W_s$  is the weight of the dry sand.

### 2.2. Preparation of samples

Unreinforced and fiber-reinforced samples were prepared using a moist tamping technique. This technique is commonly used in laboratory studies of fiber-reinforced sand and allows the control of sample density while preventing the segregation of fibers (Ibraim and Fourmont, 2007). The maximum dry density of samples decreases with increasing fiber content  $P_f$ , and samples with a higher fiber content require more compaction for a given dry

Table 1  
Characteristics of polypropylene fiber.

Fiber type	Length (mm)	Diameter (mm)	Specific gravity, $G_f$	Tensile strength (Mpa)	Elasticity modulus (Mpa)	Fusion point (°C)	Burning point (°C)	Dispersibility
Single	12	0.034	0.91	350	3500	165	590	Excellent



Fig. 2. An overall view of the ring-shear apparatus DPRI-Ver.5.

density. In order to maintain uniform dry densities, lower dry density/higher void ratios were used in this test. A maximum value of fiber content is required to keep dry sand density and sample volume unchanged for a given void ratio, and this value increases with increasing void ratio. Three different initial void ratios after consolidation and four different percentages of fiber – 0.2, 0.4, 0.6, and 0.8% – were chosen for this investigation. A moisture content of 10% was used for the mixing process of all the test specimens. The details of the void ratios at the end of vertical consolidation, dry sand density, density grade, and fiber contents of mixtures are presented in Table 2.

In the preparation of all samples, the required water was first added into the dry sand, and then the proposed content of fibers was mixed in small increments by hand to obtain a uniform mixture. It is important to ensure that all fibers are mixed thoroughly. After that, the mixtures were divided into four equal parts, and each part was put into the shear box and compacted. Samples for this study with a height of 8 cm were prepared in four layers of equal height to achieve the proposed densities. The sample was directly formed in the testing apparatus.

### 2.3. Apparatus and testing procedure

#### 2.3.1. Ring-shear apparatus

The undrained ring-shear apparatus used in this study is the DPRI-Ver.5 which was developed at the Disaster Prevention Research Institute (DPRI), Kyoto University (Sassa, 1997, Sassa et al., 2003a,b, 2004). The overall view of the equipment and a cross section of the undrained shear box are presented in Fig. 2 and Fig. 3, and some of the main features of this apparatus are listed in Table 3. The shearing box has an inner diameter of 12 cm, an outer diameter of 18 cm and a maximum height of sample of 10.9 cm. This type of ring-shear apparatus enable us to examine the shear behavior of samples with large shear displacement when they were subjected to static or dynamic loadings under drained or undrained conditions (Sassa et al., 2004). It automatically records the normal stress, effective normal stress, pore pressure, shear resistance and other related data. Further details of the structure, control system and application of this apparatus were given by Sassa et al. (2003a,b, 2004). Wang and Sassa (2002) analyzed post-failure mobility of saturated sand through the undrained load-controlled ring-shear tests. Wang et al. (2007) studied the shearing behavior of saturated

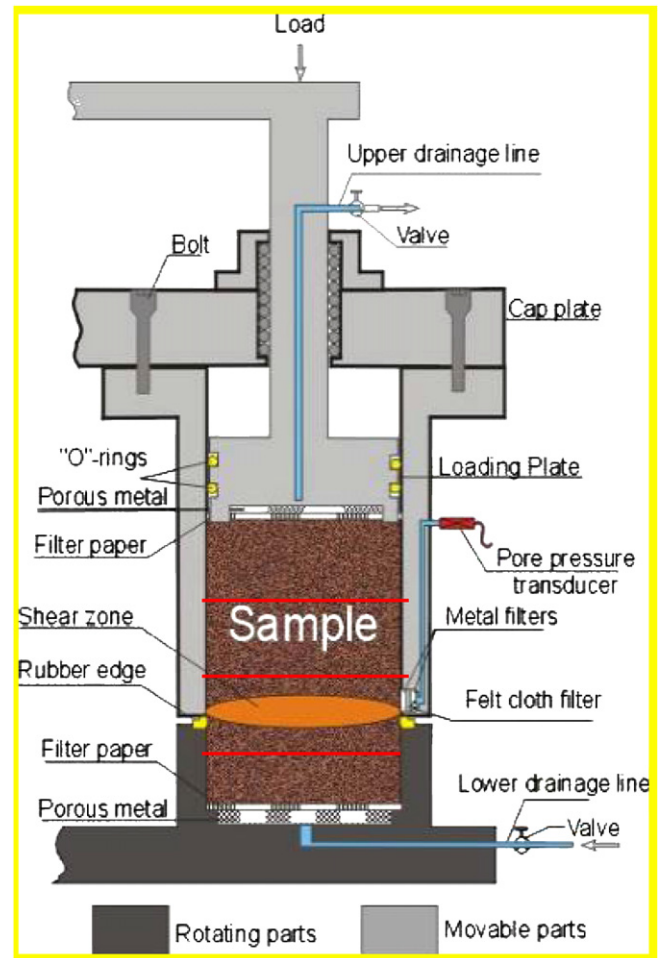


Fig. 3. A cross section of the undrained shear box.

silty soils based on the ring-shear tests. In this study, we used the undrained ring-shear apparatus to study the static liquefaction behavior of unreinforced and fiber-reinforced sand under undrained conditions.

#### 2.3.2. Testing procedure

After the sample was formed, it was saturated using carbon dioxide ( $\text{CO}_2$ ) and de-aired water. Firstly,  $\text{CO}_2$  was percolated through the sample to expel the air in the sample pores. Then, de-aired water was infiltrated into the sample to expel the  $\text{CO}_2$  as completely as possible. After that, the degree of saturation was checked using the parameter  $B_D = \Delta u / \Delta \sigma$ , where  $\Delta u$  is an increment of pore pressure and  $\Delta \sigma$  is an increment of normal stress (Sassa, 1988). In this study, the sample was first consolidated under a normal stress of 50 kPa at the drained condition. An increment of

Table 3  
The main features of the ring-shear apparatus (DPRI-Ver.5).

Shear box	
Inner diameter (cm)	12.0
Outer diameter (cm)	18.0
Max. height of sample (cm)	11.5
Ratio of max. height/width	3.83
Shear area (cm <sup>2</sup> )	141.37
Max. normal stress (kPa)	2000
Max. shear speed (cm/sec)	10.0
Cyclic torque control testing (max. frequency)	Yes (5 Hz)
Undrained testing and pore pressure monitoring	Yes
Max. data acquisition rate (readings/sec)	200

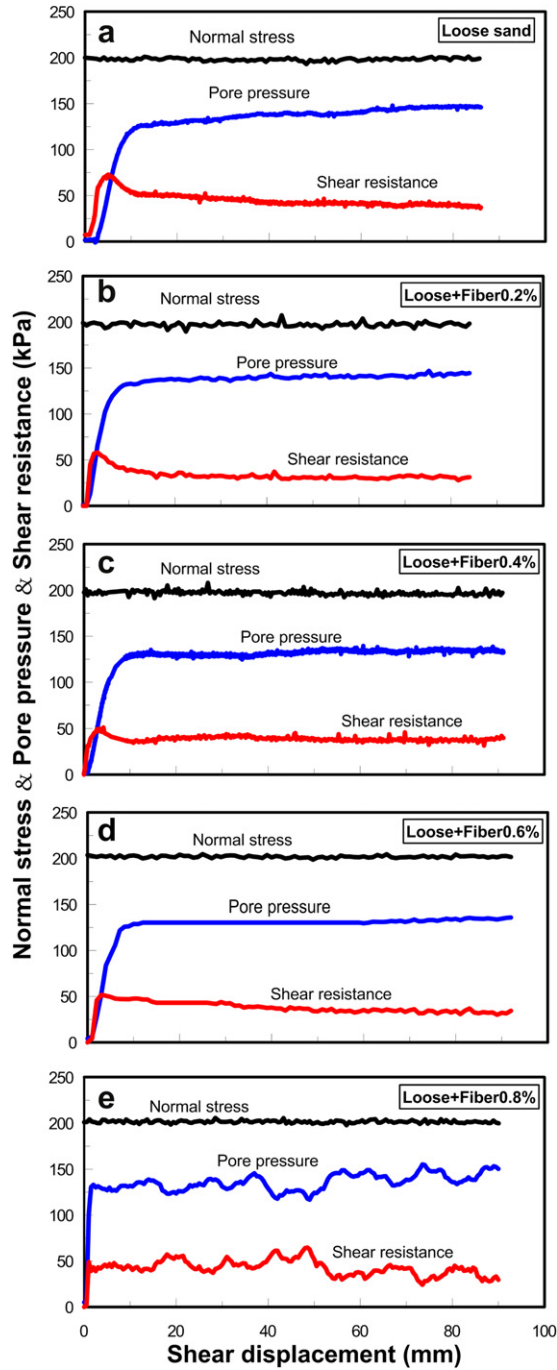


Fig. 4. Normal stress, pore pressure and shear resistance against shear displacement for loose samples with different fiber contents.

normal stress,  $\Delta\sigma = 50$  kpa, was then applied in the undrained state, and the resultant excess pore pressure increment  $\Delta u$  was measured. Finally the saturation degree  $B_D$  was indirectly given by  $\Delta u/\Delta\sigma$ . Values of  $B_D$  of at least 0.95 were deemed to indicate sufficient water saturation for all the undrained tests.

After checking the  $B_D$ , the saturated sample was consolidated under selected values of normal stress 200 kpa in a drained condition until the axial strain was constant. Thereafter, the drainage valve was closed and undrained shearing was carried out with a constant value of 1 mm/s and the shear resistance, pore pressure, shear displacement and vertical displacement were measured.

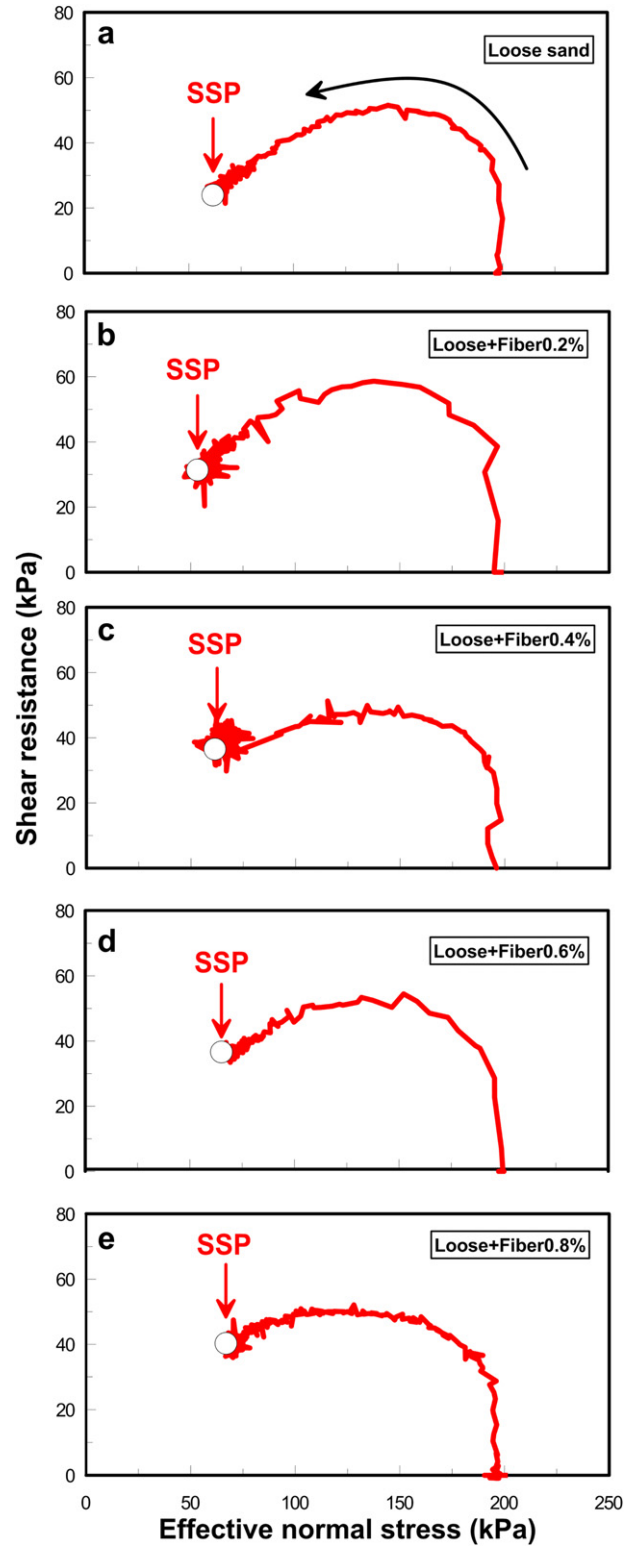


Fig. 5. Effective stress paths of loose specimens.

### 3. Experimental results

In order to discuss the results of the ring-shear tests on the saturated fiber-reinforced sand, the samples have been divided into three groups (loose, medium dense and dense states), according to their undrained shear behavior (see the note in Table 2). In the

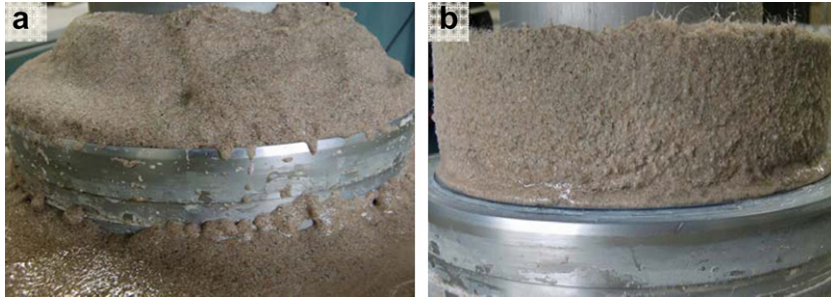


Fig. 6. Two photos of fully liquefied loose specimens after shearing: (a) Sand; (b) fiber 0.4%.

following sections the results of these three density grades of unreinforced and reinforced samples are presented.

### 3.1. Loose samples

The normal stress, pore pressure and shear resistance against shear displacement for loose specimens with different fiber contents are presented in Fig. 4 and the effective stress paths are presented in Fig. 5. As seen in Fig. 4a–d, the trends of change in pore pressure and shear resistance are fairly similar for unreinforced and reinforced samples with fiber contents of 0.2%, 0.4% and 0.6%. In the initial shearing period, the shear resistance showed a sharp increase to peak shear strength and then underwent a quick reduction, subsequently decreasing slowly until it reached a steady state. The pore pressure built up quickly and then increased gradually until it reached a steady state accompanying further shearing. Compared with the above results, the curves for 0.8% fiber-reinforced samples (Fig. 4e) show a different trend after the peak value, i.e., the pore pressure and shear resistance fluctuate. As shown in Fig. 5, the effective stress paths of the unreinforced and reinforced specimens show similar trends. Soon after the start of shearing, with increasing shear stress, the stress path moved leftwards until it reached a final steady state point (Point SSP in Fig. 5). Fig. 6 shows pictures of the fully liquefied loose specimens. The unreinforced sample clearly shows a completely collapsed structure (see Fig. 6a), while the reinforced sample still maintains structural stability even after removal of the upper ring (see Fig. 6b). It seems that the presence of fibers can limit or even prevent the lateral spreading of the soil which is one of the consequences of liquefaction. This phenomenon in triaxial undrained tests on saturated sand was also presented by Ibraim et al. (2010).

### 3.2. Medium dense samples

Fig. 7 shows the normal stress, pore pressure and shear resistance against shear displacement for the medium dense samples. The presence of fiber clearly affected the change in trends of pore pressure and shear resistance. For the unreinforced sample (Fig. 7a), at the start of shearing the shear resistance increased sharply until it reached peak shear strength and some pore pressure built up, and then decreased quickly due to the dilatancy of the sand. The fiber-reinforced samples showed the same change trends as the unreinforced sand before reaching peak shear strength. Thereafter, the reinforced samples, unlike the unreinforced sand, showed a fluctuating decrease in shear resistance for some time after shear failure, until they finally fell to a relative steady state (see in Fig. 7b–e). The fluctuations were stronger with increasing fiber content.

The effective stress path of unreinforced and reinforced samples with a medium density is shown in Fig. 8. As seen in Fig. 8a for

unreinforced sand, with an increase of shear time the effective stress path extended upward to the left due to pore pressure generation. After that, the pore pressure decreased due to the dilatancy of the sample, and the path went right upward during further shearing and showed the shape of an “elbow” with a turning point. After failure, the path fell downward until reaching a small shear stress along the residual failure line. It is noted that this kind of post shear behavior at large shear displacement was not usually obtained in triaxial tests, due to the limitations of triaxial apparatus in shear displacement. As shown in Fig. 8b–e, the fiber-reinforced samples showed a similar effective stress path, but between peak and steady state the path showed some fluctuations. The fluctuations became stronger with increasing fiber content, especially in the 0.6% and 0.8% fiber samples. Photographs of fully liquefied medium dense samples that were unreinforced or contained 0.4% fiber are showed in Fig. 9. The unreinforced sample shows a partly collapsed structure (see Fig. 9a), while the reinforced one still maintains structural stability (see Fig. 9b). This structural stability is also shown in all medium dense samples.

### 3.3. Dense samples

The results for unreinforced and reinforced dense specimens are presented in Fig. 10 and Fig. 11. As seen in Fig. 10, the presence of fiber also affected the trends of change of pore pressure and shear resistance. At the start of shearing, the shear resistance of the unreinforced sample showed a quick increase until reaching peak shear strength and then decreased continuously to reach the steady state. The pore pressure dropped down before the peak shear strength, and thereafter increased gradually until reaching a steady state. As shown in Fig. 10b–e, the change in trend of shear resistance and pore pressure of the reinforced samples were the same as for unreinforced sand before reaching peak shear strength, but after that showed some fluctuation and finally fell to a relative steady state. As shown in Fig. 11, the effective stress path is similar for unreinforced and reinforced samples: the path showed a sharp increase at the beginning and extended right upward with a turning point with further shearing, and then fell downward until reaching a small shear stress. But as the shear resistance fell, the reinforced samples showed some fluctuations (see in Fig. 11b–e). Fig. 12 shows photographs of the fully liquefied high-density specimens that were unreinforced and reinforced with 0.4% fiber. Both of them showed a good structural stability. It seems that the densification and fiber reinforcement both can limit or even prevent the occurrence of lateral spreading of the soil due to static liquefaction.

The failure shear strength, peak shear strength and residual shear strength of the unreinforced and reinforced specimens with three different densities are showed in Figs. 13–15. It should be noted that failure shear strength ( $\tau_f$ ) here refers the shear strength

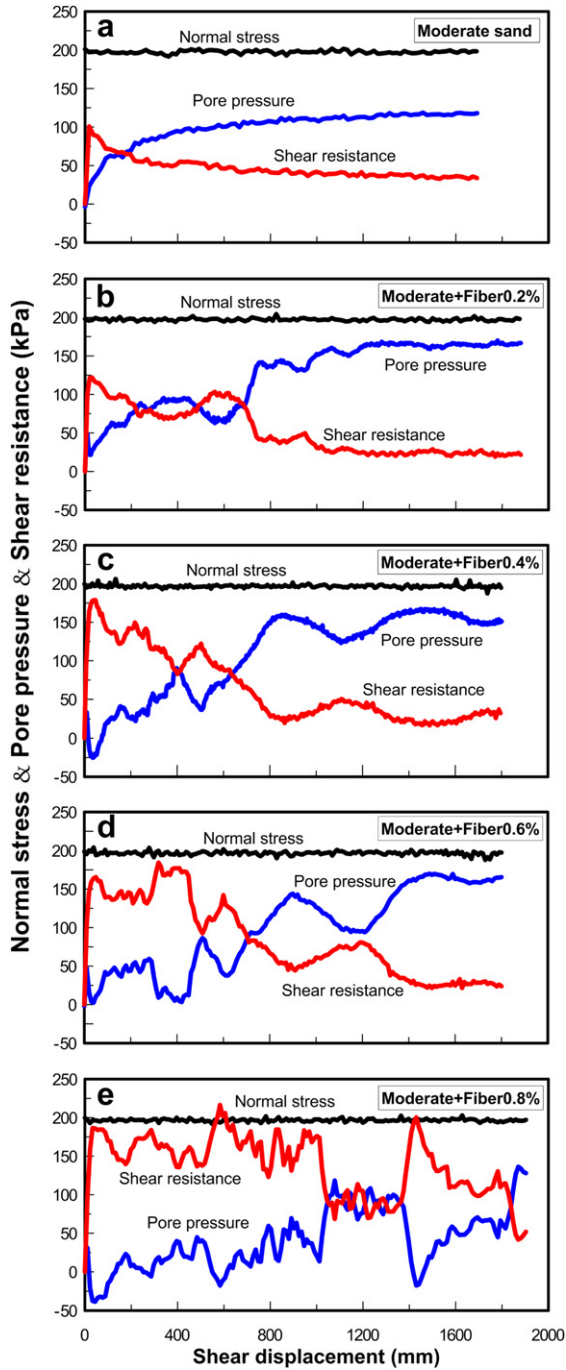


Fig. 7. Normal stress, pore pressure and shear resistance against shear displacement in medium dense specimens with different fiber contents.

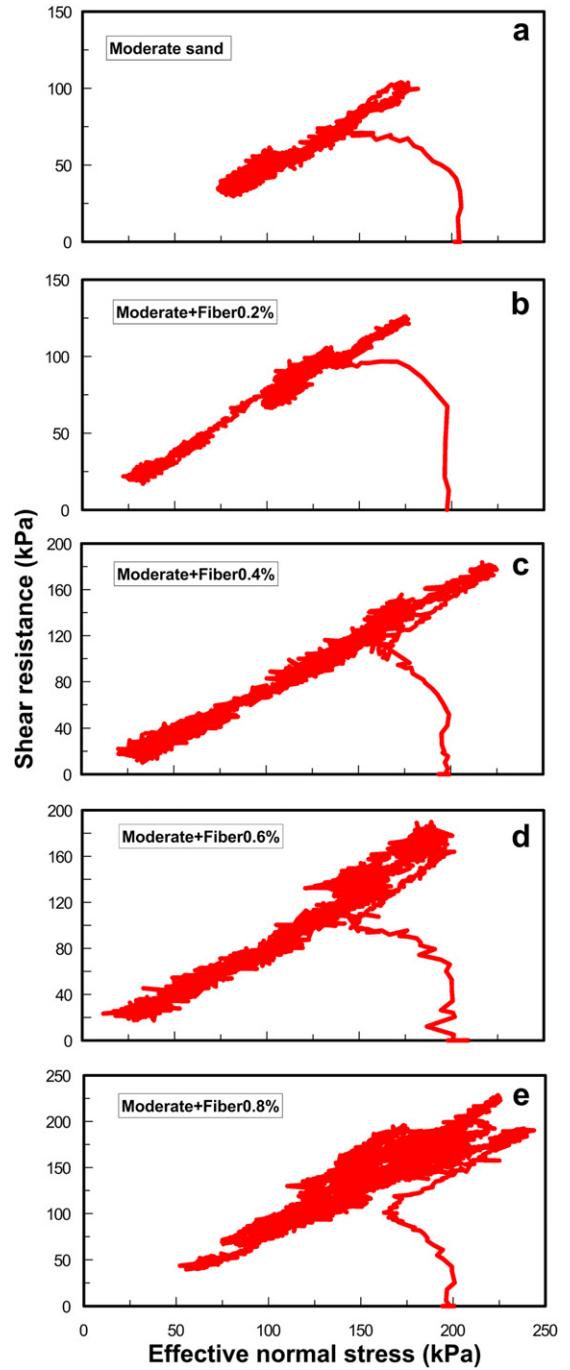


Fig. 8. Effective stress paths of medium dense samples.

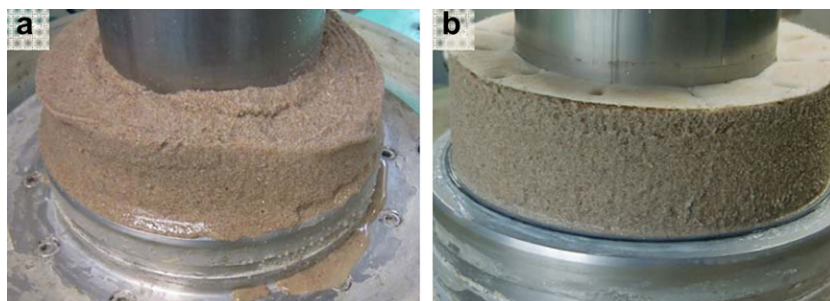


Fig. 9. Two photos of fully liquefied medium dense samples after shearing: (a) Sand; (b) fiber 0.4%.

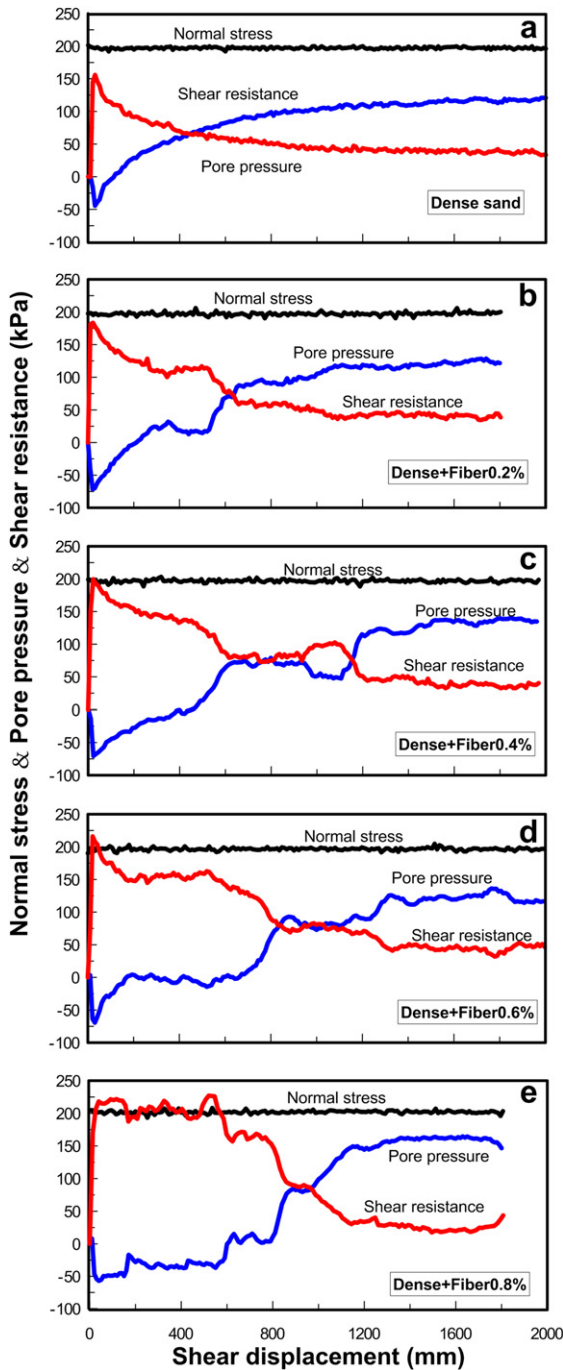


Fig. 10. Normal stress, pore pressure and shear resistance against shear displacement in dense specimens with different fiber contents.

at which the specimen begins to suffer shear failure, but the peak strength ( $\tau_p$ ) is the highest shear strength during the shearing process. For in the tests on pure sands,  $\tau_f = \tau_p$ . As shown in Figs. 13 and 14, the failure and peak shear strength is not much affected by reinforcement in loose specimens, but increases with the fiber content in medium dense and dense samples. And the peak shear strength also increases with increasing dry sand density for the same fiber content. Comparing the failure shear strength, the peak shear strength is changed in the samples with greater fiber content. It can be seen from Fig. 15 that the presence of fiber has negligible effects on the residual shear strength of samples with different densities.

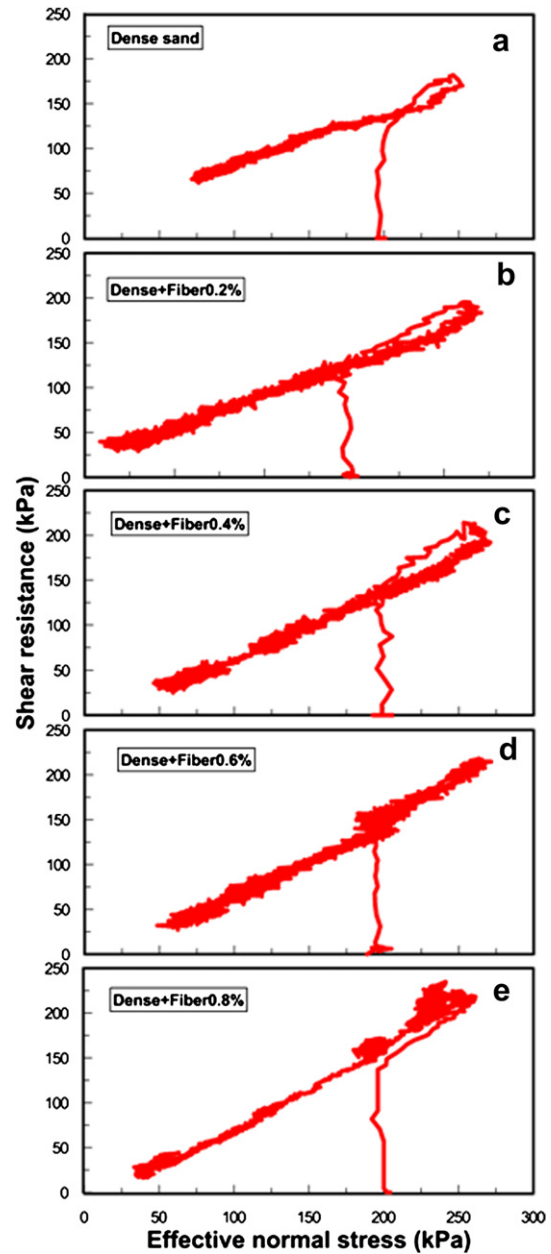


Fig. 11. Effective stress paths of dense samples.

#### 4. Discussion

The distributed fibers might act as a spatial three-dimensional network to interlock soil grains, helping the grains to form a unitary coherent matrix and restricting the displacement. Several researchers reported that the fiber surface roughness strongly affected the fiber sliding resistance (Frost and Han, 1999; Tagnit-Hamou et al., 2005; Tang et al., 2007). As the fiber was mixed or samples were compacted, the hard sand particles impacted and abraded the fiber surface, resulting in plastic deformation and even removal of part of the surface layer. It is speculated that pits and grooves that formed on the fiber surface constituted an interlock and improved the interactions between the fiber surface and the sand matrix. These interfacial mechanical interactions between the fiber and sand are greatly dependent on the sand dry density and fiber content. Loose sand corresponds to a higher void ratio and larger pore diameters. It is speculated that when the sample was

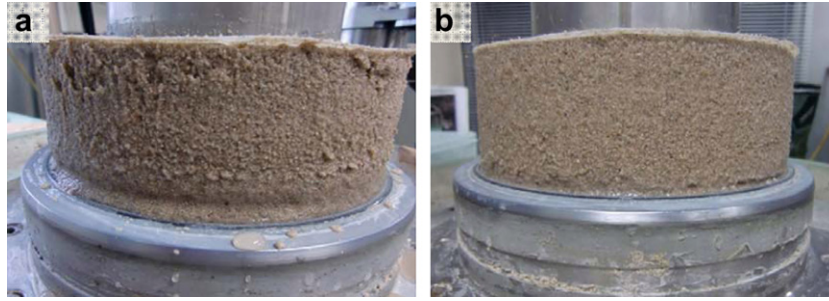


Fig. 12. Two photos of fully liquefied dense specimens after shearing: (a) Sand; (b) fiber 0.4%.

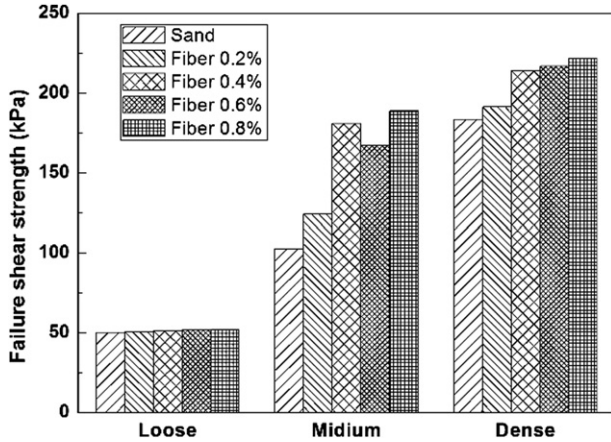


Fig. 13. The failure shear strength of unreinforced and reinforced samples with three different densities.

saturated, some of fiber was separated from the sand particles. After the sample shearing, the fiber can move easily and has no effect on the static liquefaction behavior of the saturated specimens. Furthermore, the fiber occupies only a part of the volume of sample pores in low density samples, so the low fiber content hardly changes the shearing behavior of the saturated sand. But the presence of fiber still improves the structural stability and prevents the lateral spreading of sand due to static liquefaction.

An increase of sand density gives rise to a more effective interfacial contact area between the fiber and the sand matrix. In the process of preparing samples, more compaction should be applied to obtain a high density, and this will result in a larger contact force

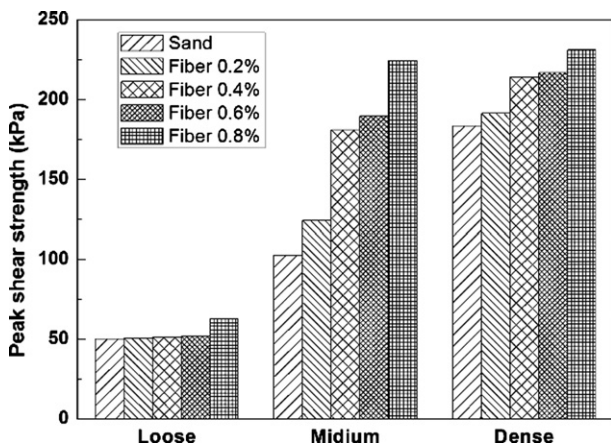


Fig. 14. The peak shear strength of unreinforced and reinforced samples with three different densities.

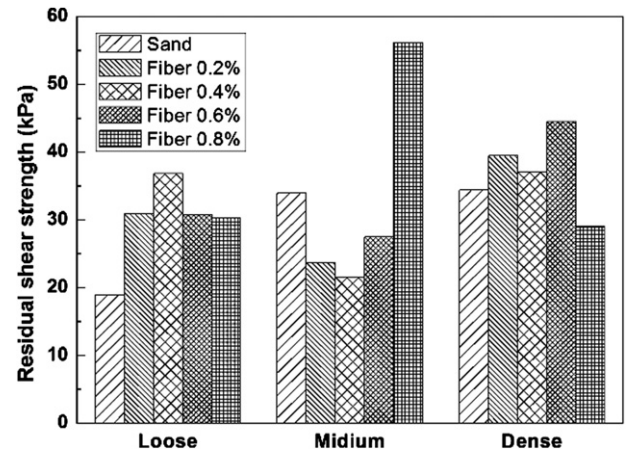


Fig. 15. The residual shear strength of unreinforced and reinforced samples with three different densities.

and interlock between adjacent sand particles and a greater plastic deformation and roughness of the fiber surfaces. Meanwhile, the interlock effect increases with the content of fiber. So the peak shear strength of samples increased with the fiber content. During ring shearing, the interfacial friction strongly depends on the resistance of sand particles to rearrangement and rotation. Normally, if sand particles are less likely to be rearranged during shearing or are more interlocked, this leads to a higher interfacial resistance to shear (Frost and Han, 1999), and if the resistance offered by mechanical interlocking between the particles and fiber surface is larger than that between adjacent sand particles, it will result in sand particle rotation (Tang et al., 2010). It is speculated that the fiber is re-oriented gradually due to the sand rearrangement and rotation in the shearing process, and this fiber orientation in a shear zone might lead to the volume expanding, the pore pressure decreasing and the shear resistance increasing. These orientations increase with the fiber content. So the fluctuation in shear resistance occurred more frequently when the fiber content increased in medium and dense samples in this study.

### 5. Conclusions

A series of ring-shear tests were performed to study the static liquefaction behavior of sand reinforced with short polypropylene fiber. The effects of the fiber content and sand density on the static liquefaction behavior of the fiber-reinforced sand were investigated. The main conclusions from the present study can be summarized as follows:

- (1) The ring-shear test provides an efficient analysis tool for evaluating the static liquefaction behavior of fiber-reinforced sand. The ring-shear apparatus used in this study can measure

the entire process of undrained shear even after sample failure and check the shear behavior at large shear displacements.

- (2) The undrained shear behavior of fiber-reinforced loose sand is not significantly influenced by the presence of fiber, but the unreinforced samples after shearing clearly show a completely collapsed structure, while the reinforced samples still maintain structural stability even after the removal of the upper ring. It seems that the presence of fibers can limit or even prevent the occurrence of the lateral spreading of sand as normally observed for unreinforced sand.
- (3) The presence of fibers clearly affects the undrained behavior of medium dense and dense samples. The results show that the test on sand showed a continued decrease in shear resistance after failure, while those treated with fiber showed fluctuations even after shear failure. This fluctuation becomes stronger with increasing fiber content. All the medium dense and dense reinforced samples maintained structural stability after shearing, while the unreinforced medium dense sample showed a partly collapsed structure and the dense sample showed structural stability. It seems that densification and fiber reinforcement both can limit or even prevent the occurrence of lateral spreading of the soil due to static liquefaction.
- (4) The failure shear strength and peak shear strength increases with the fiber content, especially for medium dense and dense samples. And they also increase with increasing dry sand density for the same fiber content. The presence of fiber has negligible effects on the residual shear strength of specimens with different densities.
- (5) The results of this investigation indicated that fiber reinforcement is useful for improving the static liquefaction resistance of sand, and the sand density and fiber content must be considered in practical applications. Further study will be performed to examine the cyclic shear behavior.

## Acknowledgments

This research is financially supported by the Natural Science Foundation of China (Grant No. 40672181), the State Key Program of National Natural Science of China (Grant No. 40730739) and the Scientific Research Foundation of Graduate School of Nanjing University (Grant No. 2009CL10). The authors gratefully acknowledge Dr. Chaosheng Tang in School of Earth Sciences and Engineering, Nanjing University, China, and Dr. Hiroshi Fukuoka, Associate Professor in Research Center on Landslides, Disaster Prevention Research Institute, Kyoto University, Japan, for their help and comments on this work. The authors are grateful to Mrs Eileen McSaveney in GNS, New Zealand for her suggested corrections to improve this paper. The authors would also like to acknowledge the editors and reviewers of this paper for their very helpful comments and valuable remarks.

## References

- Al Refeai, T.O., 1991. Behaviour of granular soils reinforced with discrete randomly oriented inclusions. *Geotextiles and Geomembranes* 10, 319–333.
- Boominathan, A., Hari, S., 2002. Liquefaction strength of fly ash reinforced with randomly distributed fibers. *Soil Dynamics and Earthquake Engineering* 22, 1027–1033.
- Castro G., 1969. Liquefaction of Sands. Ph.D. Thesis, Harvard Soil Mechanics Series, N81, Harvard University, Cambridge, MA.
- Chen, C.W., Loehr, J.E., 2009. Undrained and drained triaxial tests of fiber-reinforced sand. *Geosynthetics in Civil and Environmental Engineering* 2, 114–120.
- Consoli, N.C., Casagrande, M.D.T., Prietto, P.D.M., Thome, A., 2003. Plate load test on fiber-reinforced soil. *Journal of Geotechnical & Geoenvironmental Engineering* 129 (10), 951–955.
- Consoli, N.C., Casagrande, M.D.T., Coop, M.R., 2007. Performance of a fiber-reinforced sand at large shear strains. *Géotechnique* 57 (9), 751–756.
- Consoli, N.C., Casagrande, M.D.T., Thome, A.R., Fahey, M., Dall'ara, F., 2009a. Effect of relative density on plate loading tests on fibre-reinforced sand. *Géotechnique* 59, 471–476.
- Consoli, N.C., Vendruscolo, M.A., Fonini, A., Dalla Rosa, F., 2009b. Fiber reinforcement effects on sand considering a wide cementation range. *Geotextiles and Geomembranes* 27 (3), 196–203.
- Diambra, A., Russell, A.R., Ibraim, E., Muir Wood, D., 2007. Determination of fiber orientation distribution in reinforced sands. *Géotechnique* 57 (7), 623–628.
- Diambra, A., Ibraim, E., Muir Wood, D., Russell, A.R., Bennani, Y., 2008. Effect of sample preparation on the behaviour of fibre reinforced sands. In: Proceedings of the 4th Int. Symposium on Deformation Characteristic of Geomaterials. ISAtlanta 2008, vol. 2. IOS Press, USA, pp. 629–636.
- Diambra, A., Ibraim, E., Muir Wood, D., Russell, A.R., 2010. Fibre reinforced sands: experiments and modelling. *Geotextiles and Geomembranes* 28, 238–250.
- Frost, J.D., Han, J., 1999. Behavior of interfaces between fiber-reinforced polymers and sands. *Journal of Geotechnical and Geoenvironmental Engineering* 125 (8), 633–640.
- Heineck, K.S., Coop, M.R., Consoli, N.C., 2005. Effect of microreinforcement of soils from very small to large shear strains. *Journal of Geotechnical and Geoenvironmental Engineering* 131 (8), 1024–1033.
- Ibraim, E., Diambra, A., Muir Wood, D., Russell, A.R., 2010. Static liquefaction of fibre reinforced sand under monotonic loading. *Geotextiles and Geomembranes* 28, 374–385.
- Ibraim, E., Fourmont, S., 2007. Behaviour of sand reinforced with fibres. In: Ling, Callisto, Leshchinsky, Koseki (Eds.), *Soil Stress-strain Behaviour: Measurement, Modelling and Analysis*, Geotechnical Symposium, Rome, March 16–17. Springer, pp. 807–918.
- Jewell, R.A., Wroth, C.P., 1987. Direct shear tests on reinforced sand. *Geotechnique* 37 (1), 53–68.
- Kaniraj, S.R., Gayathri, V., 2003. Geotechnical behavior of fly ash mixed with randomly oriented fiber inclusions. *Geotextiles and Geomembranes* 21, 123–149.
- Krishnaswamy, N.R., Isaac, N.T., 1994. Liquefaction potential of reinforced sand. *Geotextiles and Geomembranes* 13 (1), 23–41.
- Li, G.X., Chen, L., Zheng, J.Q., Jie, Y.X., 1995. Experimental study on fiber-reinforced cohesive soil. *Shuili Xuebao*. *Journal of Hydraulic Engineering* 6, 31–36 (in Chinese).
- Li, J., Ding, D.W., 2002. Nonlinear elastic behaviour of fiber-reinforced soil under cyclic loading. *Soil Dynamics and Earthquake Engineering* 22, 977–983.
- Li, A.L., Rowe, R.K., 2008. Effects of viscous behavior of geosynthetic reinforcement and foundation soils on the performance of reinforced embankments. *Geotextiles and Geomembranes* 26, 317–334.
- Long, P.V., Bergado, D.T., Abuel-Naga, H.M., 2007. Geosynthetics reinforcement application for tsunami reconstruction: evaluation of interface parameters with silty sand and weathered clay. *Geotextiles and Geomembranes* 25 (4–5), 311–323.
- Maher, M.H., Ho, Y.C., 1994. Mechanical properties of kaolinite/fiber soil composite. *Journal of Geotechnical Engineering Division, ASCE* 120 (8), 1381–1393.
- Maher, M.H., Woods, R.D., 1990. Dynamic response of sands reinforced with randomly distributed fibers. *Journal of Geotechnical Engineering, ASCE* 116 (7), 1116–1131.
- Maher, M.H., Ho, Y.C., 1993. Behavior of fiber-reinforced cemented sand under static and cyclic loads. *Geotechnical Testing Journal* 16 (3), 330–338.
- Michalowski, R.L., 2008. Limit analysis with anisotropic fiber-reinforced soil. *Géotechnique* 58 (6), 489–501.
- Michalowski, R.L., Cermák, J., 2002. Strength anisotropy of fiber-reinforced sand. *Computers and Geotechnics* 29, 279–299.
- Noorany, I., Uzdevaines, M., 1989. Dynamic behavior of saturated sand reinforced with geosynthetic fabrics. In: Proc., *Geosynthetics 89 Conf*, vol. II, pp. 385–396. San Diego, California.
- Palmeira, E.M., Milligan, G.W.E., 1989. Large scale direct shear tests on reinforced soil. *Soils and Foundations* 29 (1), 18–30.
- Park, T., Ann Tan, S., 2005. Enhanced performance of reinforced soil walls by the inclusion of short fiber. *Geotextiles and Geomembranes* 23, 348–361.
- Prabakar, J., Sridhar, R.S., 2002. Effect of random inclusion of sisal fiber on strength behaviour of soil. *Construction and Building Materials* 16 (2), 123–131.
- Ranjan, G., Vasani, R.M., Charan, H.D., 1994. Behaviour of plastic fibre-reinforced sand. *Geotextiles and Geomembranes* 13 (8), 555–565.
- Ranjan, G., Vasani, R.M., Charan, H.D., 1996. Probabilistic analysis of randomly distributed fiber-reinforced soil. *Journal of Geotechnical Engineering* 122 (6), 419–426.
- Rowe, R.K., Li, A.L., 2002. Behaviour of reinforced embankments on soft rate-sensitive soils. *Géotechnique* 52 (1), 29–40.
- Rowe, R.K., Taechakumthorn, C., 2008. Combined effect of PVDs and reinforcement on embankments over rate-sensitive soils. *Geotextiles and Geomembranes* 26 (3), 239–249.
- Sadek, S., Najjar, S.S., Freiha, F., 2010. Shear strength of fiber-reinforced sands. *Journal of Geotechnical and Geoenvironmental Engineering* 136 (3), 490–499.
- Santoni, R.L., Webster, S.L., 2001. Airfields and road construction using fiber stabilization of sands. *Journal of Transportation Engineering* 127 (2), 96–104.
- Santoni, R.L., Tingle, J.S., Webster, S.L., 2001. Engineering properties of sand-fiber mixtures for road construction. *Journal of Geotechnical and Geoenvironmental Engineering* 127 (3), 258–268.
- Sassa, K., 1988. Geotechnical model for the motion of landslides. Special lecture of 5th international symposium on landslides. *Landslides* 1 (10–15), 37–55.

- Sassa, K., 1997. A new intelligent-type dynamic-loading ring-shear apparatus. *Landslide News* 10 (33).
- Sassa, K., Fukuoka, H., Wang, G., Ishikawa, N., 2004. Undrained dynamic-loading ring-shear apparatus and its application to landslide dynamics. *Landslides* 1, 7–19.
- Sassa, K., Wang, G., Fukuoka, H., 2003a. Performing undrained shear tests on saturated sands in a new intelligent type of ring-shear apparatus. *Geotechnical Testing Journal* 26 (3), 257–265.
- Sassa, K., Fukuoka, H., Wang, G., Naohide, I., 2003b. Undrained dynamic-loading ring-shear apparatus and its application to landslide dynamics. *Landslides* 1, 7–19.
- Tagnit-Hamou, A., Vanhove, Y., Petrov, N., 2005. Microstructural analysis of the bond mechanism between polyolefin fibers and cement pastes. *Cement and Concrete Research* 35 (2), 364–370.
- Tang, C., Shi, B., Gao, W., Chen, F., Cai, Y., 2007. Strength and mechanical behaviour of short polypropylene fiber reinforced and cement stabilized clayey soil. *Geotextiles and Geomembranes* 25, 194–202.
- Tang, C., Shi, B., Zhao, L., 2010. Interfacial shear strength of fiber reinforced soil. *Geotextiles and Geomembranes* 28, 54–62.
- Tingle, J.S., Santoni, R.L., Webster, S.L., 2002. Full-scale field tests of discrete fiber-reinforced sand. *Journal of Transportation Engineering* 128 (1), 9–16.
- Unnikrishnan, N., Rajagopal, K., Krishnaswamy, N.R., 2002. Behaviour of reinforced clay under monotonic and cyclic loading. *Geotextiles and Geomembranes* 20, 117–133.
- Vercueil, D., Billet, P., Cordary, D., 1997. Study of the liquefaction resistance of a saturated sand reinforced with geosynthetics. *Soil Dynamics and Earthquake Engineering* 16, 417–425.
- Wang, G., Sassa, K., 2002. Post-failure mobility of saturated sands in undrained load-controlled ring shear tests. *Canadian Geotechnical Journal* 39 (4), 821–837.
- Wang, G., Sassa, K., Fukuoka, H., Tada, T., 2007. Experimental study on the shearing behavior of saturated silty soils based on ring shear tests. *Journal of Geotechnical and Geoenvironmental Engineering, ASCE* 133 (3), 319–333.
- Wasti, Y., Butun, M.D., 1996. Behaviour of model footing on sand reinforced with discrete inclusions. *Geotextiles and Geomembranes* 14, 575–584.
- Yetimoglu, T., Inanir, M., Inanir, O.E., 2005. A study on bearing capacity of randomly distributed fibre-reinforced sand fills overlying soft clay. *Geotextiles and Geomembranes* 23, 174–183.
- Yetimoglu, T., Salbas, O., 2003. A study on shear strength of sands reinforced with randomly distributed discrete fibers. *Geotextiles and Geomembranes* 21, 103–110.
- Zornberg, J.G., 2002. Discrete framework for limit equilibrium analysis of fiber-reinforced soil. *Géotechnique* 52 (8), 593–604.